EPJ Web of Conferences **199**, 04008 (2019) https://doi.org/10.1051/epjconf/201919904008
MESON 2018

Triangle singularity enhancing isospin violation in $D_s^+ \to \pi^+\pi^0 f_0(980)$ and $\bar{B}_s^0 \to J/\psi\pi^0 f_0(980)$ decays

Wei-Hong Liang[1,*], S. Sakai[2], Ju-Jun Xie[3], and E. Oset[2]

[1]Department of Physics, Guangxi Normal University, Guilin 541004, China
[2]Departamento de Física Teórica and IFIC, Centro Mixto Universidad de Valencia - CSIC, Institutos de Investigación de Paterna, Aptdo. 22085, 46071 Valencia, Spain
[3]Institute of Modern Physics, Chinese Academy of Sciences, Lanzhou 730000, China

Abstract. We investigate isospin violation in the $\bar{B}_s^0 \to J/\psi\pi^0 a_0(980)(f_0(980))$ and $D_s^+ \to \pi^+\pi^0 a_0(980)(f_0(980))$ reactions, which proceed via a triangle mechanism. We show that the mechanism develops a singularity around the $\pi^0 f_0(980)$ or $\pi^0 a_0(980)$ invariant mass of 1420 MeV where the $\pi^0 f_0$ and $\pi^0 a_0$ decay modes are magnified and also the ratio of $\pi^0 f_0$ to $\pi^0 a_0$ production, stressing the role of the triangle singularities as a factor to enhance isospin violation. The measurement of these reactions would bring further information into the role of triangle singularities in isospin violation and the $a_0 - f_0$ mixing in particular and shed further light into the nature of the low lying scalar mesons.

1 Introduction

Triangle singularities (TS) are capturing the attention of hadron physics. Introduced by Landau in 1959 [1], the TS stems from a mechanism that can be represented by a Feynman diagram with a loop with three propagators. Under certain circumstances which correspond to having the possibility of the process occurring at the classical level, a TS in the amplitude develops when all the intermediate particles are placed on-shell and are colinear [2]. If the internal particles have non-zero width, the amplitude with TS turns into a finite peak. The TSs are helpful in simulating a resonance, providing a mechanism for the production of particular modes in reactions, and so on. There are many such examples [3–8].

The issue of isospin violation in production of the $f_0(980)$ or $a_0(980)$ resonances, and their mixing, has been a recurrent topic. While trying to establish a "$f_0 - a_0$ mixing parameter" from different reactions, the concept had to be abandoned because it was shown that the amount of isospin violation was very much reaction dependent [9–12]. Particularly, it was shown in Refs. [11, 12] that the large isospin violation in the $\eta(1405) \to \pi^0 f_0(980)$ decay [13] was due to a TS. Since then, a search for TS enhanced isospin-violating reactions producing the $f_0(980)$ or $a_0(980)$ resonances has been initiated.

We investigate the TS and isospin violation in the $\bar{B}_s^0 \to J/\psi\pi^0 a_0(980)(f_0(980))$ and $D_s^+ \to \pi^+\pi^0 a_0(980)(f_0(980))$ reactions, where $\bar{B}_s^0 \to J/\psi\pi^0 f_0(980)$ and $D_s^+ \to \pi^+\pi^0 f_0(980)$ are isospin-suppressed while $\bar{B}_s^0 \to J/\psi\pi^0 a_0(980)$ and $D_s^+ \to \pi^+\pi^0 a_0(980)$ are isospin-allowed. Based on the notion that the $a_0(980)$ and $f_0(980)$ are generated from the interaction

*e-mail: liangwh@gxnu.edu.cn

of pseudoscalar mesons [14], the results obtained will be tied to the molecular picture of the low lying scalar mesons.

2 Formalism

Let us look first at the $D_s^+ \to \pi^+\pi^0 a_0(980)(f_0(980))$ decay. At the quark level, we have the Cabibbo-favored and color-favored decay process given in Fig. 1 (a), where the $s\bar{s}$ pair has isospin $I = 0$. The hadronization of $s\bar{s}$, shown in Fig. 1 (b), can produce a K meson and a $\bar{K}^*$ meson. When we look at the $D_s^+ \to \pi^+ K\bar{K}^*$ decay, we have the partial decay width for the $D_s^+ \to \pi^+ K^+ K^{*-}$ decay,

$$\frac{\mathrm{d}\Gamma_{D_s^+\to\pi^+K^+K^{*-}}}{\mathrm{d}M_{\mathrm{inv}}(K^+K^{*-})} = \frac{1}{(2\pi)^3}\frac{p_{\pi^+}\tilde{p}_{K^{*-}}}{4m_{D_s^+}^2}C^2 p_{\pi^+}'^2, \tag{1}$$

where p_{π^+} is the π^+ momentum in the D_s^+ rest frame, $\tilde{p}_{K^{*-}}$ and p'_{π^+} are the momenta of K^{*-} and π^+ in the K^+K^{*-} rest frame, C is a common factor containing contributions from the weak vertex in Fig. 1, determined by fitting the experimental data for the branching ratio $\mathrm{BR}(D_s^+ \to \pi^+ K^+ K^{*-})$ [15, 16].

In order to produce the $a_0(980)$ or $f_0(980)$ in the final state, we look at the decay products $\pi^0\eta$ and $\pi^+\pi^-$ of the $a_0(980)$ and $f_0(980)$ respectively. The mechanism to produce the $a_0(980)$ is depicted in Fig. 2, involving a triangle diagram. The sum of the two diagrams is constructive for $\pi^0\pi^0\eta$ production via $\pi^0 a_0$ and destructive for $\pi^0\pi^+\pi^-$ production via $\pi^0 f_0$. In the case of $m_{K^+} = m_{K^0}$ and $m_{K^{*-}} = m_{\bar{K}^{*0}}$, the sum of diagrams in Fig. 2 for $\pi^0 f_0$ production would cancel and we would have exact $I = 0$ ($\pi^0 a_0(980)$) production, corresponding to the original $\bar{s}s$ state, and no $I = 1$ ($\pi^0 f_0(980)$) production. When we take the physical masses for K and $\bar{K}^*$ mesons, we get two sources of isospin symmetry breaking, from the $K\bar{K} \to \pi^0\eta$ ($\pi^+\pi^-$) amplitudes, when they are evaluated with the actual K masses, and from the loop function of Fig. 2, which is different for the two diagrams thanks to the different K masses (also $\bar{K}^*$). The interesting thing is that we can now tune the invariant mass of $\pi^0 a_0$ ($\pi^0 f_0$) by changing the energy of the emitted π^+, and for a certain value of this invariant mass, we get a TS that enhances the production of both $\pi^0 a_0$ and $\pi^0 f_0$ modes. The TS will place the $K\bar{K}^*\bar{K}$ on shell in the loop integration when the momenta of the $\bar{K}^*$ and π^0 from the $\bar{K}^*$ decay have the same direction. Since the different masses of the charged and neutral kaon cause the $\pi^0 f_0(980)$ production, the on-shell contribution is the most sensitive to these differences and we expect that the TS will enhance the $\pi^0 f_0$ production versus the $\pi^0 a_0$ one.

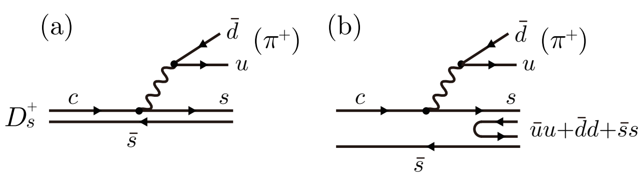

Figure 1. a) Diagrammatic representation of $D_s \to \pi^+\bar{s}s$. b) Hadronization process through $\bar{q}q$ creation with vacuum quantum number.

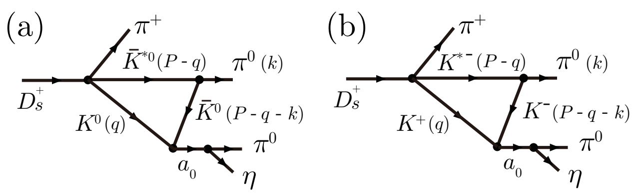

Figure 2. Triangle mechanism which produces $\pi^+\pi^0 a_0(980)$. The $\pi^+\pi^0 f_0(980)$ channel could be seen replacing $\pi^0\eta$ by $\pi^+\pi^-$ at the end. The momenta of the particles are given in the brackets.

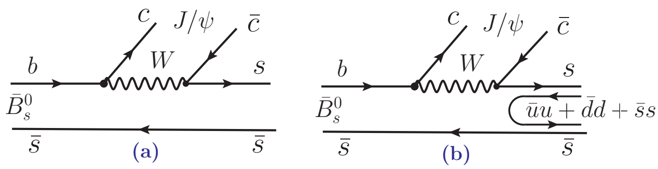

Figure 3. Diagrammatic representation of $\bar{B}_s^0 \to J/\psi(c\bar{c})s\bar{s}$ at the quark level.

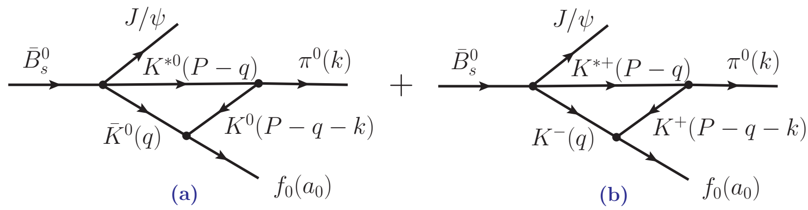

Figure 4. Triangle diagrams for the $\bar{B}_s^0 \to J/\psi\pi^0 f_0(a_0)$ decay. The parentheses give the momenta of the particles with $P = p_{\bar{B}_s^0} - p_{J/\psi}$. There are two more diagrams corresponding to (a) and (b), substituting the particles in the triangle loop with their anti-particles.

The double differential mass distribution for $D_s^+ \to \pi^+\pi^0 a_0(980)$ decay can be written as (see Ref. [17] for detail)

$$\frac{\mathrm{d}^2\Gamma_{D_s^+\to\pi^+\pi^0 a_0(980)}}{\mathrm{d}M_{\rm inv}(\pi^0 a_0)\,\mathrm{d}M_{\rm inv}(\pi^0\eta)} = \frac{1}{(2\pi)^5}\frac{p_{\pi^+} k\,\tilde{p}_\eta}{4m_{D_s^+}^2}\,|t'_{\rm eff}|^2, \tag{2}$$

where $\tilde{p}_\eta$ is the η momentum in the $\pi^0\eta$ center-of-mass frame, and

$$|t'_{\rm eff}|^2 = \frac{1}{6}C^2 g^2 p'^2_{\pi^+} k^2 \left| t_T(K^0\bar{K}^0\bar{K}^{*0})\, t_{K^0\bar{K}^0,\pi^0\eta} - t_T(K^+K^-\bar{K}^{*0})\, t_{K^+K^-,\pi^0\eta}\right|^2, \tag{3}$$

where $g = \frac{m_V}{2f_\pi}$, with $m_V \simeq 800$ MeV the vector mass and $f_\pi = 93$ MeV the pion decay constant; $t_{K^0\bar{K}^0,\pi^0\eta}$ and $t_{K^+K^-,\pi^0\eta}$ are the amplitudes for 2-body scattering processes $K^0\bar{K}^0 \to \pi^0\eta$ and $K^+K^- \to \pi^0\eta$, obtained in the chiral unitary approach [14, 18–22], and t_T is the loop function for the triangle loop in Fig. 2, given by

$$t_T = i\int \frac{d^4q}{(2\pi)^4}\frac{1}{q^2 - m_{\bar{K}^0}^2 + i\epsilon}\frac{1}{(P-q)^2 - m_{\bar{K}^{*0}}^2 + i\epsilon}\cdot\frac{1}{(P-q-k)^2 - m_{\bar{K}^0}^2 + i\epsilon}\left(2 + \frac{\vec{q}\cdot\vec{k}}{\vec{k}^2}\right). \tag{4}$$

The integrand of Eq. (4) is regularized by the three-momentum-cutoff scheme, with a cutoff $q_{\rm max} = 600$ MeV as it is needed in the chiral unitary approach that reproduces the $f_0(980)$ and $a_0(980)$ [18, 19].

For the case of $f_0(980)$ production, the formula is similar, substituting $\pi^0\eta$ in T matrices by $\pi^+\pi^-$.

For $\bar{B}_s^0 \to J/\psi\pi^0 a_0(980)(f_0(980))$ reactions, the basic diagram at the quark level is shown in Fig. 3, and the triangle diagram mechanism is shown in Fig. 4. In a similar way shown above, the double differential mass distribution for $\bar{B}_s^0 \to J/\psi\pi^0 a_0(980)$ decay can be written as (see Ref. [23] for detail)

$$\frac{1}{\Gamma_{B_s^0}}\frac{\mathrm{d}^2\Gamma_{\bar{B}_s^0\to J/\psi\pi^0 a_0(980)}}{\mathrm{d}M_{\rm inv}(\pi^0 a_0)\,\mathrm{d}M_{\rm inv}(\pi^0\eta)} = \frac{C^2}{\Gamma_{B_s^0}}\frac{g^2\, p_{J/\psi}\,\tilde{q}_\eta\,|\vec{k}|^3}{(2\pi)^5\, 8M_{B_s^0}^2}\;|t_T|^2\;\left|t_{K^0\bar{K}^0,\pi^0\eta}\right|^2\;\left|F(M_{\rm inv}(\pi^0 a_0))\right|^2, \tag{5}$$

where the function $F(M_{\rm inv}(\pi^0 a_0))$ is given by Eq. (16) of Ref. [23].

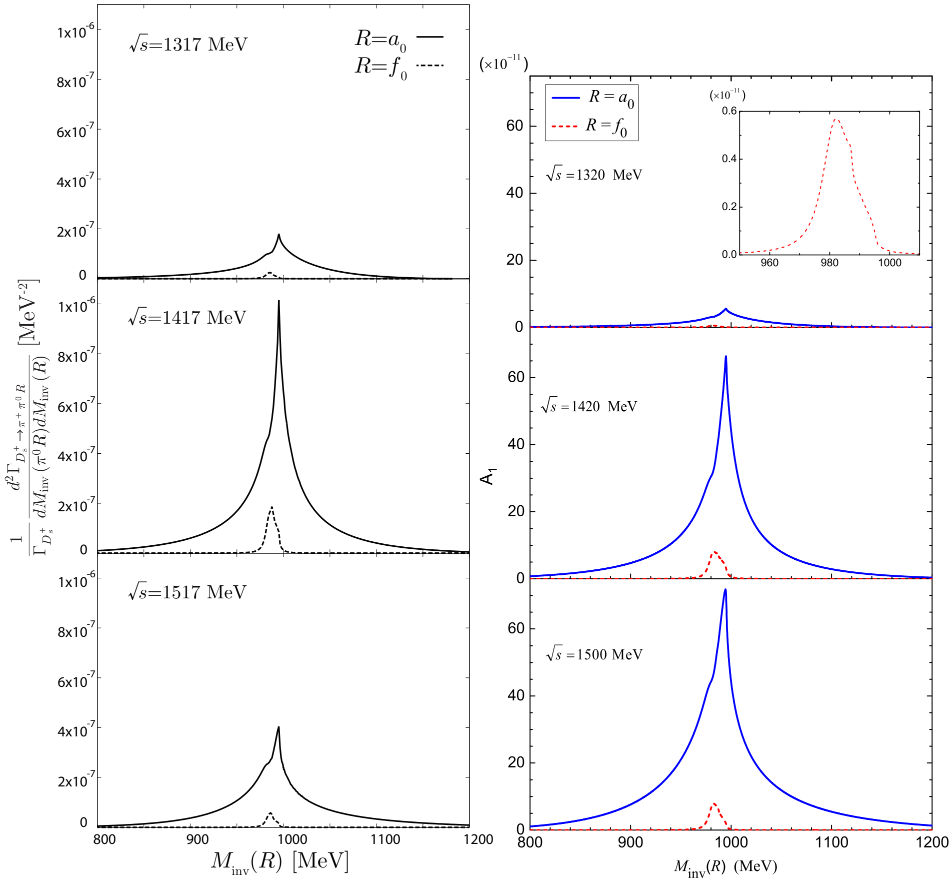

Figure 5. $\frac{1}{\Gamma_{D_s^+}}\frac{d^2\Gamma_{D_s^+\to\pi^+\pi^0 R}}{dM_{\rm inv}(\pi^0 a_0)\,dM_{\rm inv}(\pi^0\eta)}$ (left) and $\frac{1}{\Gamma_{\bar{B}_s^0}}\frac{d^2\Gamma_{\bar{B}_s^0\to J/\psi\pi^0 R}}{dM_{\rm inv}(\pi^0 a_0)\,dM_{\rm inv}(\pi^0\eta)}$ (right) as functions of $M_{\rm inv}(\pi^0\eta)$ or $M_{\rm inv}(\pi^+\pi^-)$ for three fixed values of $\sqrt{s}\equiv M_{\rm inv}(\pi^0 a_0)$ or $M_{\rm inv}(\pi^0 f_0)$. $M_{\rm inv}(R)$ for $R=a_0$ (f_0) means $M_{\rm inv}(\pi^0\eta)$ ($M_{\rm inv}(\pi^+\pi^-)$). $A_1=\frac{1}{\Gamma_{\bar{B}_s^0}}\frac{d^2\Gamma_{\bar{B}_s^0\to J/\psi\pi^0 R}}{dM_{\rm inv}(\pi^0 R)\,dM_{\rm inv}(R)}$[MeV^{-2}]. The inset in the right figure magnifies the $M_{\rm inv}(\pi^+\pi^-)$ distribution at fixed $\sqrt{s}=1320$ MeV.

3 Results and conclusion

In Fig. 5, we show the results for the double mass distribution $\frac{1}{\Gamma_{D_s^+(B_s^0)}}\frac{d^2\Gamma}{dM_{\rm inv}(\pi^0 R)\,dM_{\rm inv}(R)}$ ($R=f_0(980)$ or $a_0(980)$) of Eqs. (2) and (5) with three fixed values of $\sqrt{s}\equiv M_{\rm inv}(\pi^0 R)$. As we can see, we get two peaks for each case, corresponding to the typical $\pi^0\eta$ mass distribution of the $a_0(980)$ and the $\pi^+\pi^-$ mass distribution of the $f_0(980)$. We also observe a larger strength for $\pi^0 a_0$ production (isospin-allowed mode) than for the $\pi^0 f_0$ production (isospin-suppressed mode). However, the amount of the $\pi^0 f_0$ production is sizable. For $\sqrt{s}\sim 1420$ MeV, we get a larger strength for a_0 production as well as f_0, compared to the other two $\sqrt{s}$ energies, showing that the isospin violation is energy dependent.

In Fig. 6, we plot the ratio of $d\Gamma/dM_{\rm inv}(\pi^0 f_0)$ and $d\Gamma/dM_{\rm inv}(\pi^0 a_0)$. We see that the ratio of f_0 to a_0 production is strongly dependent on the $\pi^0 R$ ($R=f_0,a_0$) invariant mass, peaking around 1420 MeV. By going 100 MeV above and below the peak, the ratio decreases by about a factor of two and keeps decreasing as we go further away from the peak.

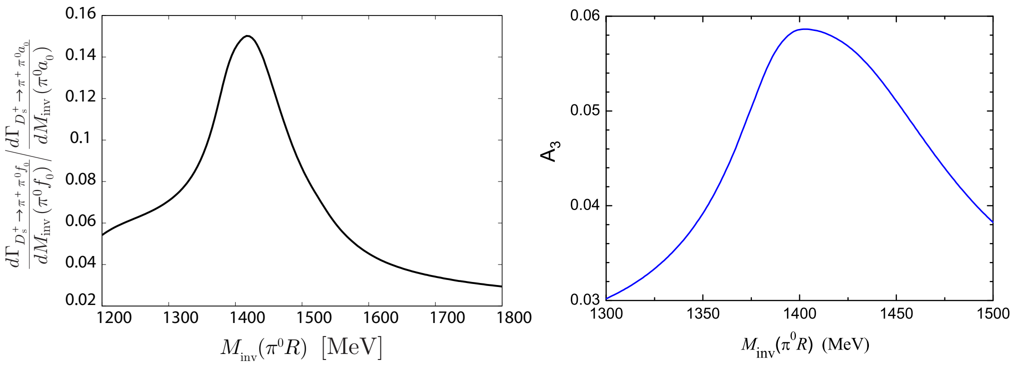

Figure 6. Ratio of $\mathrm{d}\Gamma/\mathrm{d}M_{\rm inv}(\pi^0 f_0)$ and $\mathrm{d}\Gamma/\mathrm{d}M_{\rm inv}(\pi^0 a_0)$ as a function of $M_{\rm inv}(\pi^0 R)$ ($R = f_0, a_0$), for $D_s^+ \to \pi^+\pi^0 R$ (left) and $\bar{B}_s^0 \to J/\psi\pi^0 R$ (right). $\mathrm{A}_3 = \frac{\mathrm{d}\Gamma_{\bar{B}_s^0\to J/\psi\pi^0 f_0}}{\mathrm{d}M_{\rm inv}(\pi^0 f_0)} \Big/ \frac{\mathrm{d}\Gamma_{\bar{B}_s^0\to J/\psi\pi^0 a_0}}{\mathrm{d}M_{\rm inv}(\pi^0 a_0)}$.

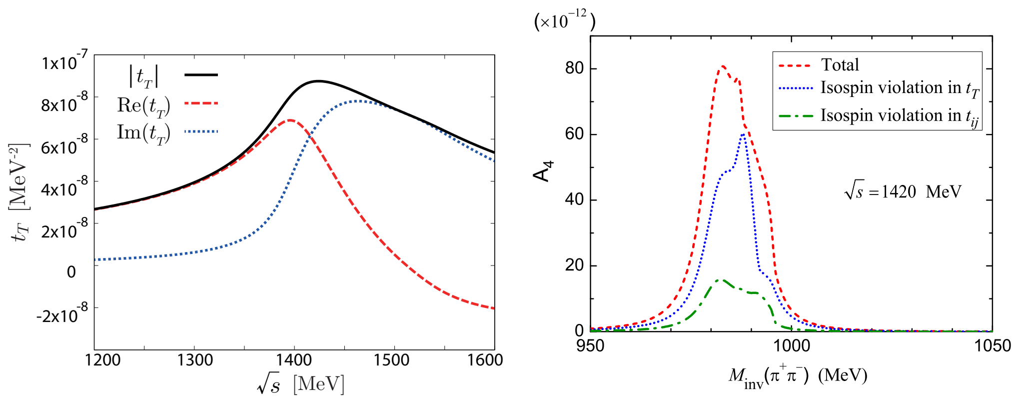

Figure 7. Left: $\mathrm{Re}(t_T)$, $\mathrm{Im}(t_T)$ and $|t_T|$ of Eq. (4). Right: $\frac{1}{\Gamma_{\bar{B}_s^0}} \frac{\mathrm{d}^2\Gamma_{\bar{B}_s^0\to J/\psi\pi^0\pi^0\eta}}{\mathrm{d}M_{\rm inv}(\pi^0 f_0)\,\mathrm{d}M_{\rm inv}(\pi^+\pi^-)}$ for fixed $M_{\rm inv}(\pi^0 f_0) =$ 1420 MeV, for two cases, isospin violation only in t_T and isospin violation only in $K\bar{K} \to \pi^+\pi^-$. $\mathrm{A}_4 = \frac{1}{\Gamma_{\bar{B}_s^0}} \frac{\mathrm{d}^2\Gamma_{\bar{B}_s^0\to J/\psi\pi^0 f_0}}{\mathrm{d}M_{\rm inv}(\pi^0 f_0)\,\mathrm{d}M_{\rm inv}(\pi^+\pi^-)}$ [MeV^{-2}].

To understand the results in Fig. 5 and Fig. 6, we plot in Fig. 7 (left) the triangle loop function t_T of Eq. (4) as a function of $\sqrt{s} \equiv M_{\rm inv}(\pi^0 a_0)$, taking for $M_{\rm inv}(\pi^0\eta)$ (or $M_{\rm inv}(\pi^+\pi^-)$) the value of 980 MeV. The peak of $\mathrm{Re}(t_T)$ appears because of the $\bar{K}^{*0}K^0$ threshold, while the one of $\mathrm{Im}(t_T)$ comes from the TS of the triangle loop. We can see that $|t_T|$ has a peak around 1420 MeV and its origin is the TS developed by the amplitude. Clearly, it is a consequence of the TS that ratios in Fig. 6 peak at $M_{\rm inv}(\pi^0 R) \sim 1420$ MeV. This means that the TS is very effective at enhancing the isospin-violating $\pi^0 f_0$ mode.

It is interesting to see the sources of isospin violation. They are tied to the differences of m_{K^0} and m_{K^+}, but they influence both t_T with TS as well as the 2-body scattering matrices t_{ij} for $K\bar{K} \to \pi^0\eta$ and $K\bar{K} \to \pi^+\pi^-$. To show the effects independently, we calculate the $\pi^0 f_0$ production in two cases: One assuming equal K masses in t_{ij} (isospin symmetry in t_{ij}) and keeping different K masses in the t_T, and another case with equal K masses in t_T but different masses in t_{ij}. The results are shown in Fig. 7 (right), where the "Total" line contains isospin violation both in t_T and t_{ij}. We can see that both effects are important and they add to the total amplitude producing $\pi^0 f_0$.

Finally, in order to estimate the branching ratios for $D_s^+ \to \pi^+\pi^0 f_0(980)(a_0(980))$ and $\bar{B}_s^0 \to J/\psi\pi^0 f_0(980)(a_0(980))$, we integrate $\frac{d^2\Gamma}{dM_{\rm inv}(\pi^0 R)\, dM_{\rm inv}(R)}$ in Fig. 5 over $M_{\rm inv}(R)$ and $M_{\rm inv}(\pi^0 R)$, and find

$$\mathrm{Br}(D_s^+ \to \pi^+\pi^0 f_0) = 4.9 \times 10^{-4}, \qquad \mathrm{Br}(D_s^+ \to \pi^+\pi^0 a_0) = 3.9 \times 10^{-3}, \tag{6}$$

$$\mathrm{Br}(\bar{B}_s^0 \to J/\psi\pi^0 f_0) = 3.3 \times 10^{-7}, \qquad \mathrm{Br}(\bar{B}_s^0 \to J/\psi\pi^0 a_0) = 4.9 \times 10^{-6}. \tag{7}$$

These rates are within present observation capability at LHCb.

In summary, we perform calculations for the $D_s^+ \to \pi^+\pi^0 f_0(980)(a_0(980))$ and $\bar{B}_s^0 \to J/\psi\pi^0 f_0(980)(a_0(980))$ reactions, showing that the $a_0(980)$ mode is isospin-allowed while the $f_0(980)$ mode is isospin-suppressed. The triangle mechanism develops a TS around the $\pi^0 f_0(980)$ or $\pi^0 a_0(980)$ invariant mass of 1420 MeV, which enhance the isospin violation. We calculate absolute rates for the reactions and show that they are within present measurable range. The experimental measurement is encouraged, which will bring further light into the issue of $f_0(980) - a_0(980)$ mixing and the nature of the light scalar mesons.

This work is supported by the National Natural Science Foundation of China (Grants Nos. 11565007, 11747307, 11735003 and 11475227).

References

[1] L. D. Landau, Nucl. Phys. **13**, 181 (1959)
[2] S. Coleman and R. E. Norton, Nuovo Cim. **38**, 438 (1965)
[3] M. Bayar, F. Aceti, F. K. Guo and E. Oset, Phys. Rev. D **94**, 074039 (2016)
[4] X. H. Liu, M. Oka and Q. Zhao, Phys. Lett. B **753**, 297 (2016)
[5] V. R. Debastiani, F. Aceti, W. H. Liang and E. Oset, Phys. Rev. D **95**, 034015 (2017)
[6] J. J. Xie, L. S. Geng and E. Oset, Phys. Rev. D **95**, 034004 (2017)
[7] E. Wang, J. J. Xie, W. H. Liang, F. K. Guo and E. Oset, Phys. Rev. C **95**, 015205 (2017)
[8] J. J. Xie and F. K. Guo, Phys. Lett. B **774**, 108 (2017)
[9] J. J. Wu, Q. Zhao and B. S. Zou, Phys. Rev. D **75**, 114012 (2007).
[10] C. Hanhart, B. Kubis and J. R. Pelaez, Phys. Rev. D **76**, 074028 (2007).
[11] J. J. Wu, X. H. Liu, Q. Zhao and B. S. Zou, Phys. Rev. Lett. **108**, 081803 (2012).
[12] F. Aceti, W. H. Liang, E. Oset, J. J. Wu and B. S. Zou, Phys. Rev. D **86**, 114007 (2012).
[13] M. Ablikim *et al.* [BESIII Collaboration], Phys. Rev. Lett. **108**, 182001 (2012).
[14] J. A. Oller and E. Oset, Nucl. Phys. A **620**, 438 (1997) Erratum: [Nucl. Phys. A **652**, 407 (1999)]
[15] P. U. E. Onyisi *et al.* [CLEO Collaboration], Phys. Rev. D **88**, 032009 (2013)
[16] C. Patrignani *et al.* (Particle Data Group), Chin. Phys. C **40**, 100001 (2016)
[17] S. Sakai, E. Oset and W. H. Liang, Phys. Rev. D **96**, 074025 (2017)
[18] W. H. Liang and E. Oset, Phys. Lett. B **737**, 70 (2014)
[19] M. Bayar, W. H. Liang and E. Oset, Phys. Rev. D **90**, 114004 (2014)
[20] W. H. Liang, J. J. Xie and E. Oset, Phys. Rev. D **92**, 034008 (2015)
[21] W. H. Liang, J. J. Xie and E. Oset, Eur. Phys. J. C **75**, 609 (2015)
[22] W. H. Liang, J. J. Xie and E. Oset, Eur. Phys. J. C **76**, 700 (2016)
[23] W. H. Liang, S. Sakai, J. J. Xie and E. Oset, Chin. Phys. C **42**, 044101 (2018)